

DISPLACEMENT-BASED DESIGN VERSUS FORCE-BASED DESIGN FOR STRUCTURAL WALLS

MEHRDAD SASANI and DON L. ANDERSON

Department of Civil Engineering, The University of British Columbia,
Vancouver, BC, V6T 1Z4, Canada

ABSTRACT

This study looks at the dynamic elastic plastic response of structural walls of different strengths, to investigate if stronger walls perform better if measured in terms of the displacement or curvature. Considering the concrete strain concentration at the base of structural walls, the assumption that plane sections remain plane in flexure is improved. To investigate the effects of the accelerograms on the results, two sets of records have been used; sixteen records on rock and sixteen records on alluvium which the latter set has an almost linear average displacement spectrum up to a period of 3 seconds. The results show that weaker structures perform as well as, if not better than, stronger structures. The analytical method has been checked by different experimental data, and a good agreement is shown. At the end the contradiction between force and displacement-based design is discussed.

KEYWORDS

Structural walls; displacement-based design; force-based design; performance-based design; concrete structures; nonlinear dynamic analysis; moment-curvature relationship; displacement spectra; displacement ductility.

INTRODUCTION

Consider a single structural wall subjected to lateral loads. As far as the ultimate behavior of the wall is concerned, it is ultimate displacement or ultimate force that controls the performance of the wall. Assume that the strength of a structural wall, having the same concrete cross section as the first wall is increased by 50% by adding more reinforcement, and that this has negligible effect on the stiffness of the section. As shown in Fig. 1, by assigning equal displacement ductility to both walls, the stronger wall is assumed to have higher displacement capacity by the same 50%. But is this actually the case? It can be shown that, by increasing the reinforcement ratio in a section, even in both the tension and compression faces, the displacement capacity of the wall is decreased.

An attempt has been made to investigate the performance of single structural walls under severe seismic loading. The main variable is the amount of longitudinal reinforcement in the section. To take into account the effects of axial load, different levels of compressive stress are considered. To consider the effects of the periods of the structures, different height walls along with different vertical to horizontal mass ratios (m_z/m_v) have been used. Also, sections with and without boundary elements have been considered. The analytical method has been checked by different experimental results.

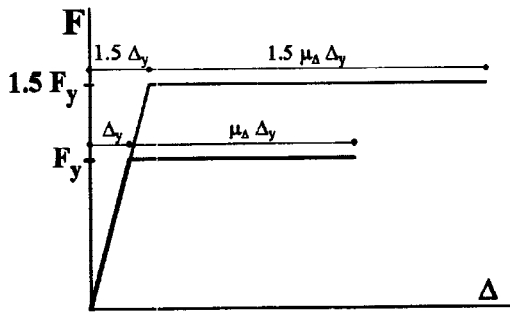


Fig. 1. Force displacement relationships for constant displacement ductility

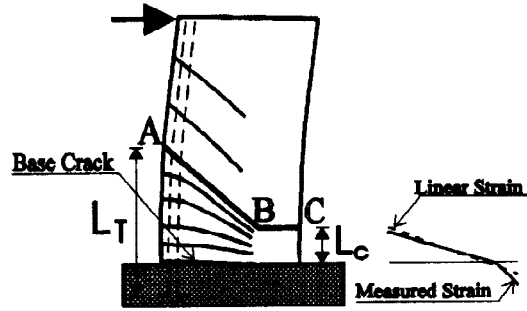


Fig. 2. Fanned radially cracked region at the bottom of a structural wall and schematic strain distribution at the base

THE FLEXURAL BEHAVIOR OF STRUCTURAL WALLS

The traditional assumption that plane sections remain plane in flexure is not applicable to structural walls within the hinging region. In Fig. 2, the schematic measured strain distribution at the base is compared to a linear one; the calculated compressive strain is considerably less than the measured strain. Based on more than twenty tests on isolated structural walls under lateral loads, with or without the presence of vertical loads, Oesterle (1986) introduced the radially "fanned" cracked pattern as a basis for developing a compatibility relationship instead of the assumption of the linear distribution of strain along the section (Fig. 2). He equates the accumulated tensile strain over the length, L_T , to that of the compressive strain over a relatively short length, L_C .

Figure 3 shows the ratio of measured to calculated (plane sections remain plane), compressive strain versus rotational ductility for four structural walls with boundary elements, termed barbell walls, (Oesterle, 1986). The boundary element reinforcement ratios for these walls are between 0.02 and 0.037. Walls B11 and B12 are under lateral loads only while walls B9 and B10 also have axial loads. The concrete strength in wall B11 (53.7 MPa) is considerably higher than that of the other walls. Based on Fig. 3, in this study it is assumed that the maximum compressive concrete strain at the base of structural walls is twice as much as the result of a section analysis based on a linear distribution of strain. This assumption is checked below by the results of other experiments.

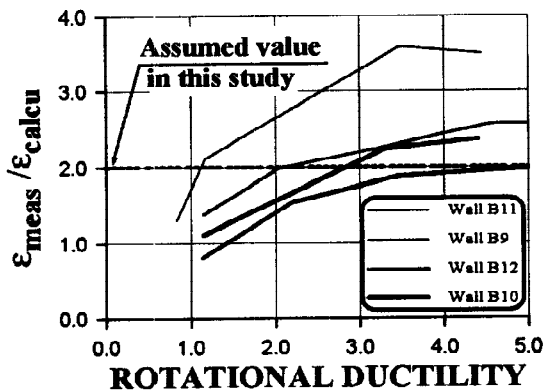


Fig. 3. Ratio of measured to calculated (linear strain distribution) compressive strain of concrete versus rotational ductility

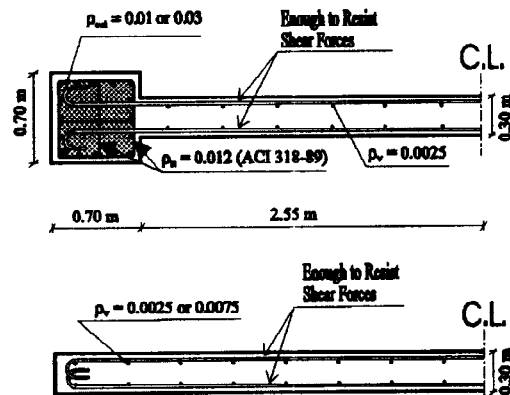


Fig. 4. Rectangular section and section with boundary elements (barbell section)

STRUCTURAL WALLS USED IN THIS STUDY

Walls of 5, 10, and 15-stories, with 3.6 m story heights, have been studied. The 5 and 10-story walls have uniformly reinforced rectangular cross sections whereas the 15-story wall has boundary elements. Fig. 4 depicts the sections and the reinforcement details. The axial load is assumed to give a compressive stress at the base level

equal to $0.05f'_c$ and $0.10f'_c$ for the 5 and 10-story walls, respectively. The compressive stress on the boundary elements of the 15-story wall is $0.30f'_c$ (the boundary elements carry all the loads). These cases are investigated for each wall by varying the horizontal masses, m_H , to be 1.0, 2.0, and 3.0 times the vertical masses, m_v . The P- Δ effects and also the shear deformation effects are not included; the Rayleigh damping of 5% in the first two modes is assumed.

IDEALIZED MOMENT-CURVATURE RELATIONSHIPS

To define an elastic-perfectly plastic behavior for sections, three parameters should be defined: flexural stiffness, ultimate curvature, and yield or ultimate strength. These parameters have been discussed in detail by Sasani (1996), and only a quick review is provided below.

Equivalent flexural stiffness, $(EI)_{eq}$, which includes contribution of both cracked and uncracked sections of the wall has been used throughout the height of the wall. Considering the concrete strain concentration at the base of a structural wall, limiting the maximum usable concrete compressive strain and the steel tensile strain, and using the computer program BIAx (Wallace, 1992), which considers the nonlinear stress strain relationship of concrete and reinforcement, the monotonic ultimate curvature of the section Φ_u is calculated. Taking into account low-cycle fatigue, as proposed by Fajfar (1992), the (cyclic) ultimate curvature of the section Φ_u is defined. Finally, ultimate flexural strength of each section is defined as shown in Fig. 5. Results, based on deformation shown in Fig. 6, are given in Table 1.

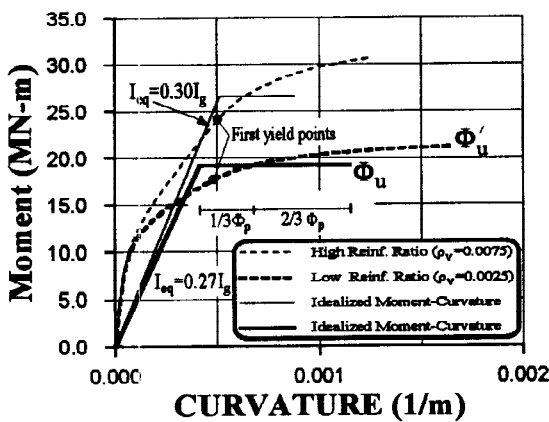


Fig. 5. Moment-curvature relationships for rectangular sections with $P=0.1 A_g f'_c$

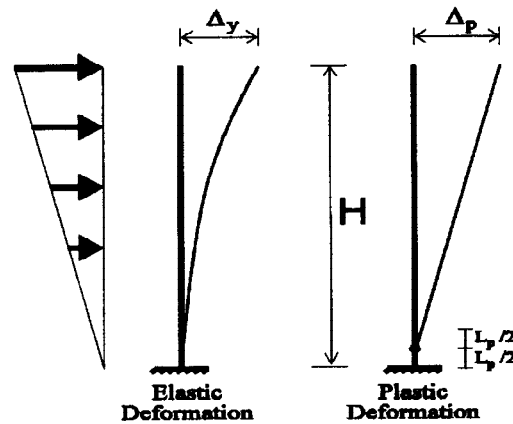


Fig. 6. The elastic and plastic deformation of walls under lateral loads

TABLE 1. The calculated properties of the sections and the structural walls in this study. (The length of all walls, the depth of sections, is 6.5 m).

	5 story wall (H=18.0 m)		10 story wall (H=36.0 m)		15 story wall (H=54.0 m)	
	$P/A_g f'_c=0.05$		$P/A_g f'_c=0.10$		$P/(2*A_{bc}f'_c)=0.30$	
ρ_w or ρ_{bc} (%)	0.25(Low)	0.75(High)	0.25(Low)	0.75(High)	1.0(Low)	3.0(high)
I_{eq}/I_g	0.24	0.26	0.27	0.30	0.32	0.45
M_u (MN-m)	11.1	18.6	19.0	26.6	43.3	70.0
Failure Mode	CC ^a	CC	CC	CC	CC	CC
μ_p (Capacity)	5.29	2.29	2.78	1.71	10.8	8.5
μ_Δ (Capacity)	3.26	1.67	1.53	1.21	3.36	2.81
D_c (m) ^b	0.094	0.075	0.228	0.224	1.38	1.30
D_c (%) ^b	0.519	0.418	0.633	0.622	2.56	2.40

^a CC= Concrete Crushing

^b Displacement capacity and Drift capacity respectively

This method has been checked by using the test results of four structural walls carried out by Cardenas *et al.* (1973), Oesterle *et al.* (1976), and Vallenias *et al.* (1979). Again the comparison is discussed in detail by Sasani (1996), and only some of the results are given in Table 2.

TABLE 2. Comparison between the experimental and the calculated results for the isolated structural walls previously tested

Specimen - monotonic loading	reference No.	I_y/I_e		Δ (m) ^b or Θ (100*rad) ^b			Displacement ductility ^b		
		Meas.	Calcu.	Meas.	Calcu. Case 1 ^c	Calcu. Case 2 ^c	Meas. (monot.)	Meas. (cyclic.)	Calcu. (cyclic.)
PCA/B4	Oesterle, (1976)	0.12	0.13	0.226	0.253	0.253	18.8	8.3	8.7
PCA/SW2	Cardenas, (1973)	0.33	0.26	0.464 ^d	0.530 ^d	0.530 ^d	N/A	N/A	N/A
UCB/SW3	Vallenias, (1979)	0.41	0.44	0.109	0.113	0.087	11.2	4.5	5.9
UCB/SW5	Vallenias, (1979)	0.43	0.50	0.050	0.064	0.057	7.7	4.2	4.6

^a The measured I_y are the average values for the lower 0.20, 0.16, 0.30, and 0.42 of total height, respectively

^b At levels 1.0, 0.16, 0.30, 0.42 of the total height, respectively (the highest levels with available data)

^c Cases 1 and 2 are based on two different eqs., to find the maximum usable concrete strain, (Sasani, 1996)

^d These values are the rotations at 0.16 of total height for specimen PCA/SW2

DRIFT CAPACITIES AND DEMANDS AND SHEAR FORCE DEMANDS

Assuming an inverted triangular distribution for the lateral load, the yield displacement at the top of the structural wall is $\Delta_y = \phi_y H^2/3.6$ if $\phi_y = M_y/EI$. Therefore the displacement capacity at the top of the structural wall is given by the following equation (Fig. 6):

$$\Delta_c^t = \frac{\Phi_y H^2}{3.6} + (\Phi_u - \Phi_y) L_p (H - L_p/2) \quad (1)$$

where ϕ_y and ϕ_u are yield and ultimate curvatures of the section. L_p is the plastic hinge length, and H is the total height of the wall (Fig. 6).

Drift capacity, D_c , is defined as the top displacement capacity divided by the total height of the wall.

Accelerograms Recorded on Rock Sites

Sixteen accelerograms with $PGA > 0.2g$ and $PGV > 0.2$ m/s having $(PGA)_{ave} = 0.47g$, $(PGV)_{ave} = 0.46$ m/s, and $(PGD)_{ave} = 0.11$ m, have been used in this study. Eight of these accelerograms were recorded in California, two of them recorded during the Central Chile earthquake (March 3, 1985), and the other six are from the San Salvador earthquake (October 10, 1986). The average and the (average + σ) displacement response spectra (for 5% damping) for these records are shown in Fig. 7.

Nonlinear time step analyses have been carried out with the elastic-plastic moment curvature relations, using the computer program DRAIN-2DX. Results in terms of D_d/D_c and V_d/V_c versus the periods of walls are shown in Figs. 8 and 9, where D_d and V_d are drift and base shear force demands, and V_c is the nominal shear resistance of the concrete section, based on ACI 318 (1989).

As can be seen in Figs. 8 and 9, in all cases both D_d/D_c and V_d/V_c for lightly reinforced sections are less than those for the more heavily reinforced sections.

As shown in Fig. 8, for 5-story walls, the slope of D_d/D_c is very steep, compared to that of the 10 and 15-story walls. This can be explained by looking at the displacement response spectra of the records (Fig. 7). As shown, the

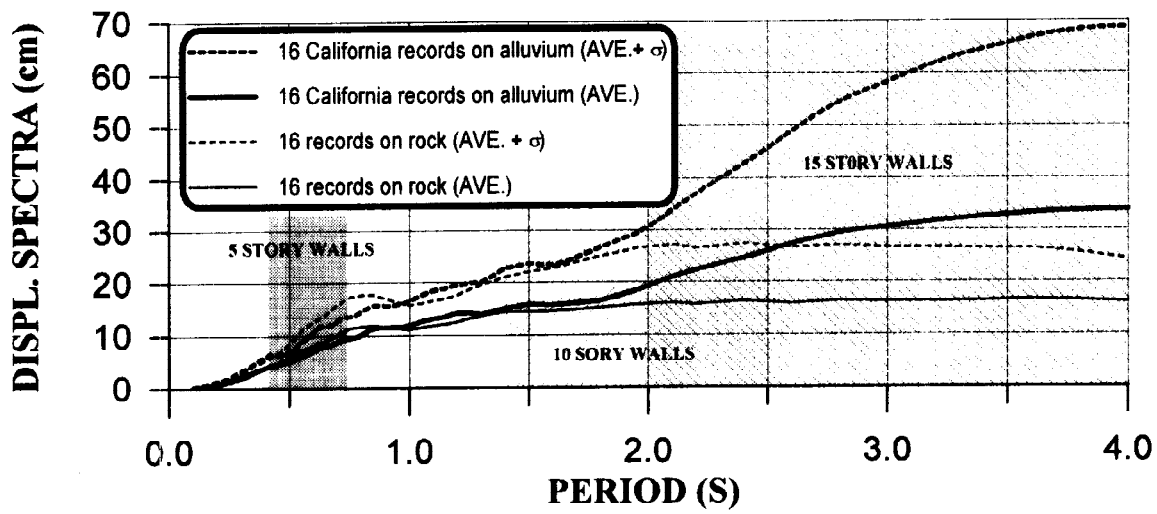


Fig. 7. Displacement response spectra for accelerograms recorded on rock and alluvium sites

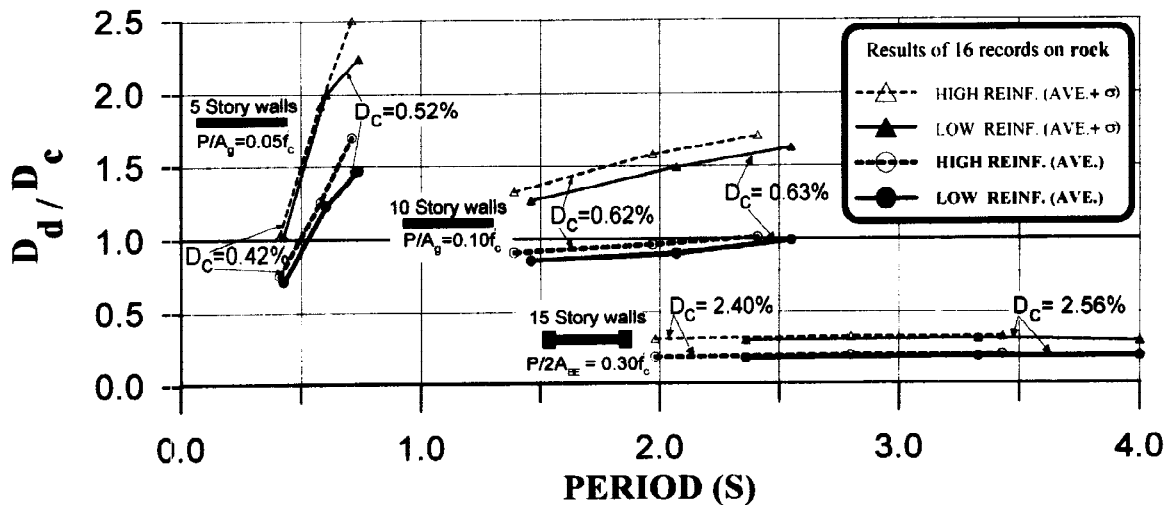


Fig. 8. Comparison between ratios of drift demand, D_d , and drift capacity, D_c , for low and high amounts of flexural reinforcement. The three points on each curve from left to right correspond to m_H/m_V equal to 1, 2, and 3, respectively

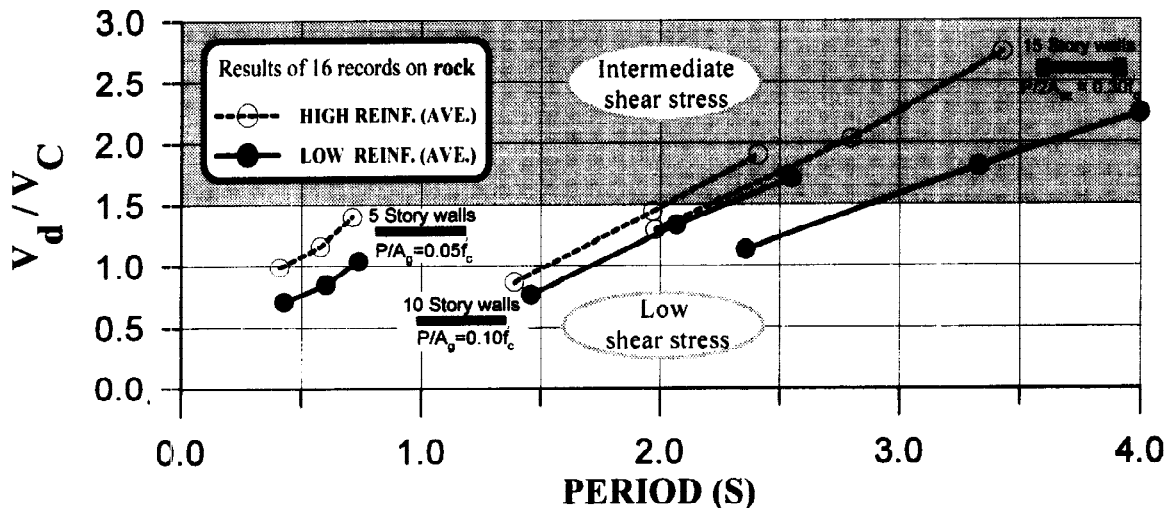


Fig. 9. Comparison between ratios of shear force demand, V_d , and nominal shear force resistance, V_c , for low and high amount of flexural reinforcement (only average results are shown)

5-story walls have fallen in the steepest region of the spectra, while the variation of the displacement spectra for the 10 and 15-story walls is more gradual.

The very small values of $(D_d/D_c)_{ave}$ for 15-story walls with barbell sections show the effectiveness and, probably, the overly conservative confinement of the boundary elements of the structural wall sections. Note the different values for drift capacity for sections with and without confined boundary elements.

By increasing the amount of reinforcement in the sections, as a result of higher ultimate base moment, the base shear force increases. Based on more than 20 lateral cyclic tests on isolated structural walls, Oesterle *et al.* (1976) have concluded that the behavior of structural walls can be categorized as follows: as low nominal shear stress walls, with predominantly flexural behavior, $V < 1.5V_C$, as intermediate shear stress walls, $1.5V_C < V < 3.0V_C$; and as high shear stress walls, $V > 3.0V_C$, with predominantly shear failure. These categorization mean that, beyond some level of base shear, shear failure is not easily prevented by providing more horizontal reinforcement and in that situation, shear failure mainly depends on the concrete cross section and its strength. Therefore, by adding more flexural reinforcement to the section as a result of higher base shear forces, brittle shear failure might occur. Figure 9 shows that although barbell sections are under higher shear forces, none of the walls considered in this study, falls into the high shear stress region.

California Accelerograms Recorded on Alluvium Sites

To provide a better understanding of the effects of the records (or their displacement spectra) in this study, in the case of alluvium sites, first, sixteen accelerograms all recorded in California are used, second, the records are chosen in such a way that their average displacement spectrum has an almost linear trend up to $T=3s$ (Fig. 7). Again, all the records have $PGA > 0.2g$ and $PGV > 0.2$ m/s, with $(PGA)_{ave} = 0.38g$, $(PGV)_{ave} = 0.44$ m/s, and $(PGD)_{ave} = 0.17$ m. The results of nonlinear dynamic analyses, in terms of D_d/D_c and V_d/V_C versus the periods of walls, are shown in Figs. 10 and 11.

As shown in Figs. 10 and 11, for 5-story walls, in all cases both D_d/D_c and V_d/V_C for lightly reinforced sections are less than those for the more heavily reinforced sections. For these walls, using records on rock and alluvium sites, the results are almost the same, which could be explained by the displacement spectra of the records, (Figs 7-11).

Although for 10 and 15-story walls, V_d/V_C for lightly reinforced sections are less than those for the more heavily reinforced sections, it is not always true for D_d/D_c . The ratios between D_d/D_c and also V_d/V_C (or simply V_d) for highly and lightly reinforced sections are given in Table 3. A value greater than one shows that the increase of reinforcement in the section has not improved the performance of the section. For 10-story walls, the average value for $(D_d/D_c)_{high\ reinf} / (D_d/D_c)_{low\ reinf}$ varies between 0.86 and 1.04 (i.e., a maximum improvement of 14% for three times increase in the reinforcement ratio of the sections). For 15-story walls, this ratio varies between 0.91 and 1.05. It should be mentioned that although in some cases increasing the main reinforcement results in some flexural improvement, it always corresponds with higher shear forces, which is not desirable.

Table 3. Comparison between results of highly and lightly reinforced sections (alluvium records)

	No of stories	Average of results			(Average + σ) of results		
		m_H/m_V			m_H/m_V		
		1	2	3	1	2	3
$(D_d/D_c)_{high\ reinf}$	5	1.15	1.04	1.12	1.09	0.97	1.09
	10	1.04	0.86	0.96	1.02	0.79	0.94
$(D_d/D_c)_{low\ reinf}$	15	0.91	0.91	1.05	0.88	0.85	1.00
$(V_d/V_C)_{high\ reinf}$	5	1.32	1.42	1.29	1.52	1.38	1.20
	10	1.10	1.09	1.14	1.05	1.16	1.20
$(V_d/V_C)_{low\ reinf}$	15	1.07	1.20	1.17	1.06	1.20	1.24

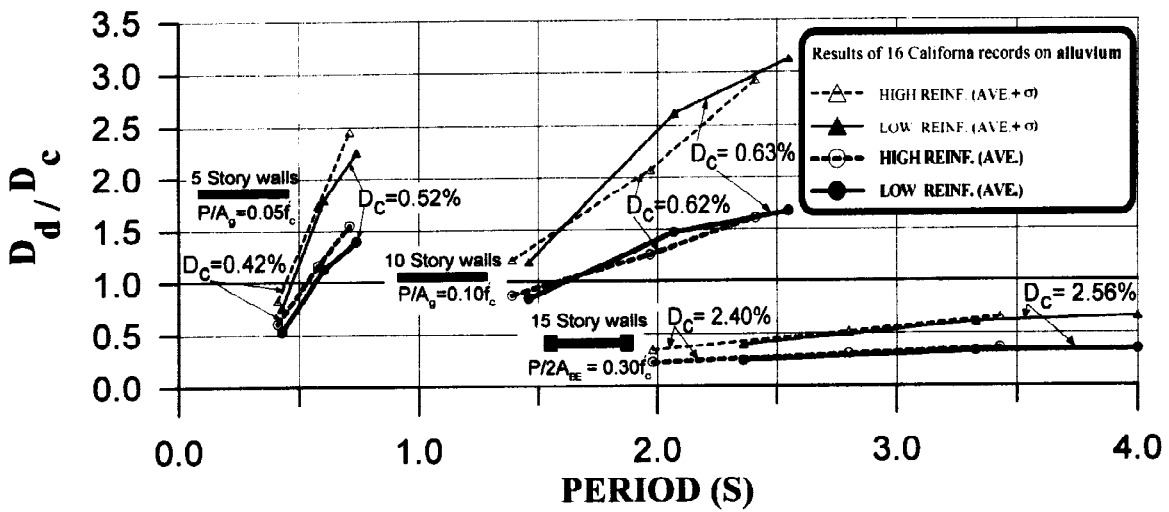


Fig. 10. Comparison between ratios of drift demand, D_d , and drift capacity, D_c , for low and high amounts of flexural reinforcement. The three points on each curve from left to right correspond to m_H/m_v equal to 1, 2, and 3, respectively

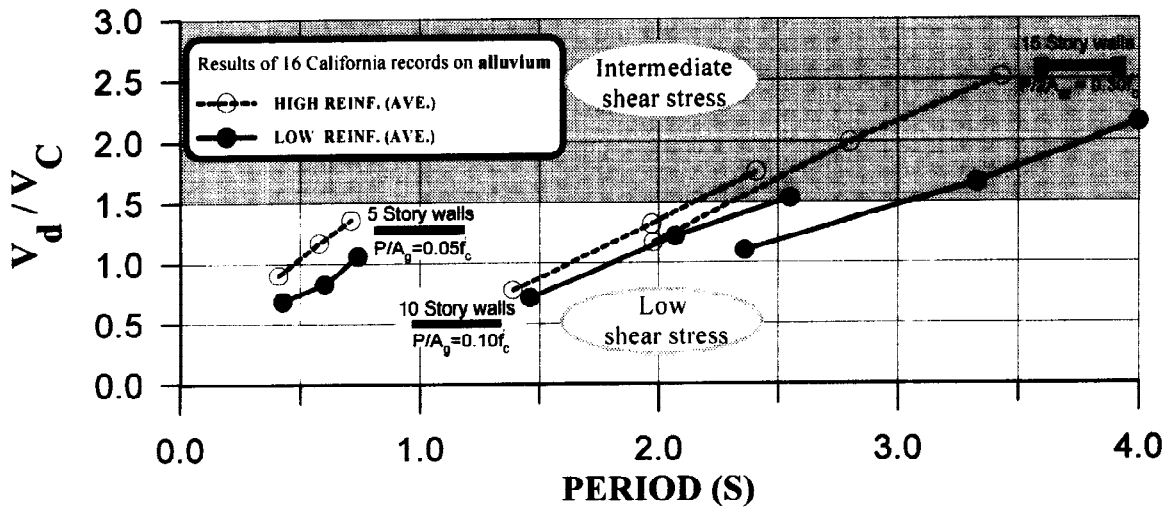


Fig. 11. Comparison between ratios of shear force demand, V_d , and nominal shear force resistance, V_c , for low and high amount of flexural reinforcement (only average results are shown)

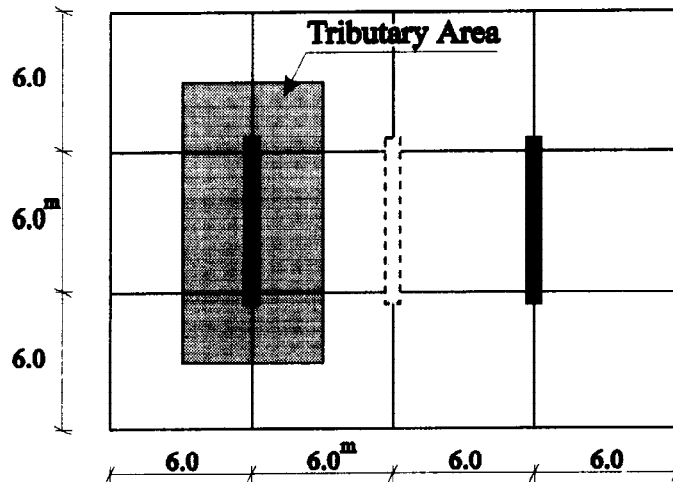


Fig. 12. Plan of a five-story building (only the lateral resisting system in one direction is shown)

FORCE-BASED DESIGN

Given the plan of a 5-story structure (Fig. 12), if one designs this structure based on the Uniform Building Code (1994), for a site with $Z=0.40$ and $S=1.35$ (the average of $S_1=1.2$ and $S_2=1.5$ to be comparable with the alluvium site used in this study), having $I=1$ and $R_w=8$, the following might be concluded: (1) having three walls in the plan, $m_H/m_V=2.0$, the design leads to the vertical reinforcement ratio, ρ_v , of 0.0025; (2) if the middle wall is removed, ($m_H/m_V=3.0$), $\rho_v=0.0025$ would not be sufficient and about 50% increase in the base moment capacity is needed. (3) designing the structure with two walls in the plan results in $\rho_v=0.0064$. In other words, from the point of view of force, comparing second and third cases, a 2.56 times increase in ρ_v would lead to the expectation of a 50% improvement in the seismic behavior of the walls, while from the displacement point of view, this increasing of the reinforcement ratio results in a 12% reduction of the flexural performance of structural walls, measured by D_d/D_c , and an increase of 29% in base shear force, neither of which is desirable.

CONCLUSION

Based on this limited investigation it is concluded that increasing strength, by adding more reinforcement to a given section, has little effect, if any, on the performance of structural walls as measured by the curvature or displacement capacity; indeed, such an increase in strength might lead to a brittle shear failure because of the absorption of higher lateral forces. Although using two different sets of records, changed the results (in terms of D_d/D_c) to some extent, it did not influence the above conclusion. Because it is not easy to explain these kinds of seismic structural performance by the traditional force-based design, perhaps the displacement-based design should be considered as a promising analysis tool in seismic design.

REFERENCES

- Building Code Requirements for Reinforced Concrete, ACI 318 (1989). ACI, Detroit, MI.
- Cardenas, A. E., and D. D. Magura (1973). Strength of high-rise shear walls – rectangular cross section. In: *Response of multistory concrete structures to lateral forces, SP-36*, pp. 119-150. ACI, Detroit, MI.
- Fajfar, P. (1992). Equivalent ductility factors, Taking into account low-cycle fatigue. *Earthquake Eng. and Struct. Dyn.* 21, 837-848.
- Oesterle, R. G. (1986). Inelastic analysis for in-plane strength of reinforced concrete shear walls. Ph.D. Dissertation, Northwestern Univ., Evanston, IL.
- Oesterle, R. G., A. E. Fiorato, L. S. Johal, J. E. Carpenter, H. E. Russell, and W. G. Corley (1976). Earthquake resistance structural walls – tests of isolated walls. CTL, PCA, Skokie, IL.
- Sasani, M. (1996). Performance based design of structural walls. Submitted for review and possible publication to *Earthquake Spectra*.
- Uniform Building Code (1994). Vol. 2. International Conference of Building Officials, Whittier, CA.
- Vallenas, J. M., V. V. Bertero, and E. P. Popov (1979). Hysteretic behavior of reinforced concrete structural walls, UCB/EERC-79/20. Civil Eng. Dept., Univ. of California, Berkeley, CA.
- Wallace, J. W. (1992). BIAx: A computer program for the analysis of reinforced concrete and reinforced masonry sections, CU/CEE-92/4. Civil Eng. Dept., Clarkson Univ., Potsdam, NY.